NUCLEAR FIELD THEORY OF SPIN DEALIGNMENT IN STRONGLY ROTATING NUCLEI AND THE VACUUM POLARIZATION INDUCED BY PAIRING VIBRATIONS

F. BARRANCO [a,b], M. GALLARDO [a,b] and R.A. BROGLIA [c,b]

[a] *Departamento de Física Atómica y Nuclear, Universidad de Sevilla, E-41080 Sevilla, Spain*

[b] *The Niels Bohr Institute, University of Copenhagen, DK-2100 Copenhagen Ø, Denmark*

[c] *Dipartimento di Fisica, Universitá di Milano, Via Celoria 16, I-20133 Milan, Italy and INFN, Sezione di Milano, I-20133 Milan, Italy*

Received 18 December 1986; revised manuscript received 19 August 1987

Processes where particles are dressed by pairing vibrations and where their average field is modified by the Fock contribution of the pairing force are found to give rise to dynamical dealignments of the single-particle motion in strongly rotating nuclei above the critical frequency. Typical values for an $i_{13/2}$ orbital are $8\hbar$, in qualitative agreement with the experimental findings.

The advent of Compton suppressed germanium detectors (cf. e.g. ref. [1] and references therein) and the development of the cranked shell model [2] have allowed for a deep probing of the properties of nuclei at high rotational frequencies.

A central question which has been pursued in these investigations is the mechanism by which nuclei can accommodate large values of the angular momentum. This problem was found to be intimately connected with the role pairing correlations play in nuclei. This is because the pairing force tries to bind pairs of particles in time reversal states, strongly reducing the ability nucleons moving in single-particle orbitals have to carry angular momentum. This results in the formation of a condensate of pairs of particles whose stability is measured by the static pairing gap.

Angular momentum will weaken pairing correlations, as the Coriolis force acts opposite on the two members of the pair. Ultimately, the Coriolis force will tend to align the particle angular momentum of the particles with the rotational axis [3].

The picture of the alignment of single-particle states provides a simple model for the collapse of the pairing gap at high spins. Excitations of states with 3–4 quasiparticles lead in general, to the disappearance of the superfluid phase. However, even at $\omega > \omega_c$ there is still an observed favouring of states where certain pairs of nucleons are coupled to spin zero, over states with other couplings [4].

Pairing fluctuations, which seem to have no or little influence on the nuclear properties at rotational frequencies smaller than the critical, have been found [5] to give rise to important ω-dependent renormalizations of the energies and alignments of different rotational bands (cf. also ref. [6]).

A convenient basis to describe these effects is provided by single-particles (fermions) and pairing vibrations (bosons). A microscopic description of the associated fields can be obtained in terms of the cranked shell model and of the random phase approximation (RPA) respectively. The interweaving of these fields lead to strong renormalization of the single-particle motion [#1], and can be treated within the framework of the nuclear field theory (NFT) [8].

In the present paper we apply the methods of NFT to shed light into the physical mechanism which is at the basis of the dealignment produced by the coupling of nucleons, moving in a rotating potential, to the pairing vibrations [9] of the system [zero point

[#1] A schematic representation of the associated dealignment process is shown in fig. 12 of ref. [7].

fluctuations (ZPF)]. We carry the study for nucleons moving in a single $i_{13/2}$ orbital at high rotational frequencies ($\omega > \omega_c$), in a formalism which conserves the number of particles [5]. That is, we only consider normal systems, well away from the critical frequency ω_c at which the normal to superfluid phase transition takes place.

The hamiltonian describing the system is

$$H = h_{sp} + H_p \ , \qquad (1)$$

where

$$h_{sp} = Qj_z^2 - \omega j_x \qquad (2)$$

is the single-particle routhian, and

$$H_p = -GP^\dagger P \qquad (3)$$

is the pairing force. The constant Q is proportional to the quadrupole moment of the system, and was set equal to 1/6. Such a choice will approximately correspond, in a realistic system, to a quadrupole deformation $\beta \sim 0.3$. The angular momentum operators along the symmetry axis and the axis of rotation are denoted j_z and j_x respectively. The quantity ω is the rotational frequency.

The pairing coupling constant is denoted G, and the pairing field is defined as

$$P^\dagger = \sum_m a_m^\dagger a_{\tilde{m}}^\dagger = \sum_{jj'} M_{j\hat{j}'} a_j^\dagger a_{\hat{j}'}^\dagger \ . \qquad (4)$$

Here the state $\tilde{m}$ is the single-particle state time reversed to m, while j is an eigenstate of (2) with signature $\alpha = 1/2$, the state $\hat{j}$ carrying opposite signature. In the subspace used in the present paper $j, = 1, ..., 7$ and similar for $\hat{j}$. For the single-particle states the basis of ref. [10] has been used, implying that m has positive signature and $\tilde{m}$ negative. The label j indicates levels above $(j=k)$ and below $(j=i)$ the Fermi energy.

The pairing matrix elements are defined by the relation

$$M_{j\hat{j}'} = \sum_m G_j^{\prime m} H_{\hat{j}'}^{\tilde{m}} \ . \qquad (5)$$

The quantities G and H are transformation coefficients between single-particle states at $\omega = 0$ and cranked states. For more details cf. refs. [7,11].

With these elements the pairing vibrations are calculated in the random phase approximation (RPA), and the Hartree–Fock and particle vibration hamiltonians constructed. Making use of the NFT rules the lowest-order corrections [#2] to the alignments shown in fig. 1 are worked out. Examples of the value of these graphs are given in the following expression:

$$\text{graph 1(e)} = -G \sum_j \frac{M_{j\hat{i}} M_{j\hat{k}} (j_x)_{ki}}{\varepsilon_k - \varepsilon_i} \ ,$$

graph 1(f)

$$= \frac{A_n^2(-2) M_{k'\hat{k}''} M_{k\hat{k}''} (j_x)_{kk'}}{[\varepsilon_{k'} + \varepsilon_{\hat{k}''} + W_n(-2)][\varepsilon_k + \varepsilon_{\hat{k}''} + W_n(-2)]} \ ,$$

graph 1(j)

$$= -2 \frac{A_n^2(-2) M_{k\hat{k}'} M_{k\hat{i}} (j_x)_{\hat{i}\hat{k}'}}{[\varepsilon_k + \varepsilon_{\hat{k}'} + W_n(-2)](\varepsilon_{\hat{k}'} - \varepsilon_{\hat{i}})} \ . \qquad (6)$$

The quantity $A_n(\beta)$ is the particle vibration coupling constant measuring the strength with which fermions couple to the nth pair addition $(\beta = +2)$ and pair subtraction $(\beta = -2)$ modes, the label β indicating the transfer quantum number. The summed number of pair addition and pair removal modes are, in the present model, seven ($n = 1, 2, ..., 7$). The single-particle routhians are defined in eq. (2). The quantities $(j_x)_{ki}$ are the matrix elements of the x-component of the angular momentum operator between the single-particle states k and i.

The standard expression for the correlation energy (cf. ref. [5]),

$$E_{corr} = \frac{1}{2} \sum_{n, \alpha = \pm 2} W_n(\alpha) - \frac{1}{2} \sum_{jj'} (\varepsilon_j + \varepsilon_{\hat{j}'}) \ , \qquad (7)$$

is the difference between the sum of the RPA energies $W_n(\beta)$ and the unperturbed two-particle or two-hole energies. Taking the derivative of this quantity with respect to the rotational frequency one obtains the contribution to the alignments induced by the coupling of nucleons to the pairing modes,

$$\langle j_x \rangle = \langle j_x^N \rangle - dE_{corr}/d\omega \ . \qquad (8)$$

Derivatives are equivalent, in the graphical language, to insertions. In fact, it is numerically shown below that the result (8) is equal to order $1/\Omega$, to the summed contribution of graphs (d)–(m) of fig. 1.

[#2] The small parameter in the perturbative expansion of the NFT is $1/\Omega$, where Ω is the effective degeneracy given to the single particle to correlate. In the present case $\Omega = j + 1/2 = 7$.

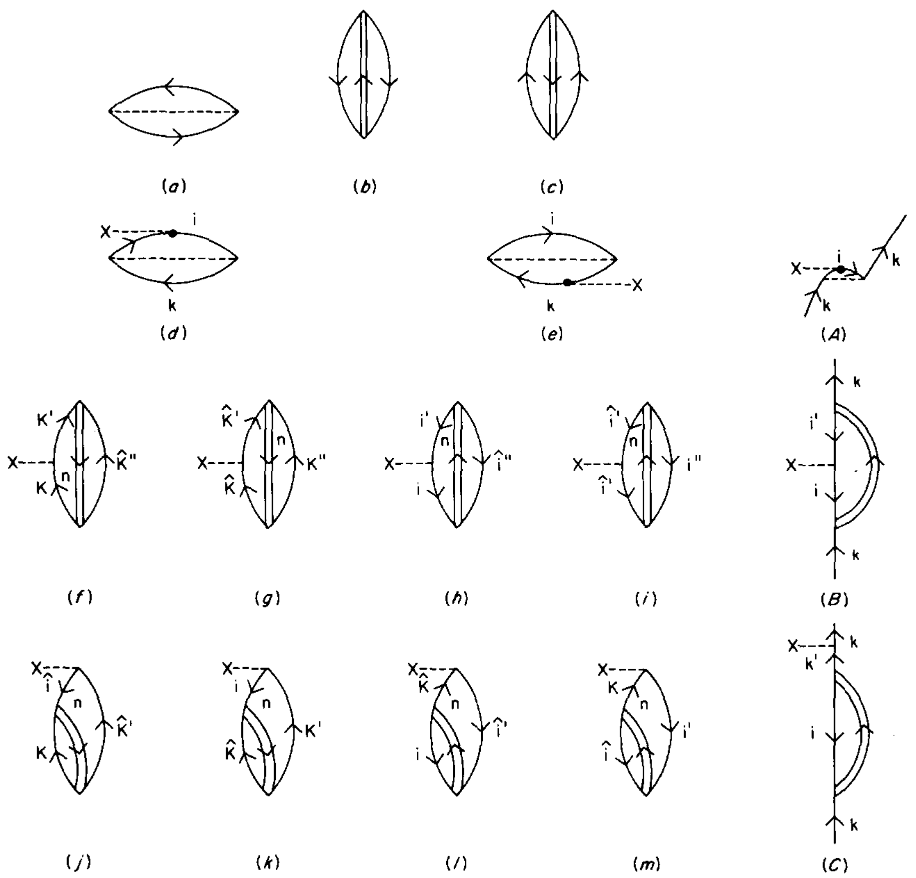

Fig. 1. Nuclear field theory diagrams describing vacuum polarization processes in lowest-order perturbation theory. An arrowed line pointing upwards labels a particle while one pointing downwards labels a hole. A double arrowed line indicates a pair addition mode (pointing up) or a pair removal mode (pointing down). A dashed internal line indicates the two-body interaction, while a dashed line ending in a cross indicates the action of the external field j_x. In (a)–(c) the vacuum polarization diagrams are indicated. In (a) the Fock contribution of the pair field to the vacuum energy is indicated, while the vacuum polarization diagrams associated with pairing vibrations (cf. ref. [11]) are shown in (b) and (c). The associated dealignment processes are shown in graphs (d), (e) and (f)–(m). The corresponding single-particle self-energy diagrams are displayed in (A), (B) and (C).

In fig. 2 the summed cranked, Fock and vacuum polarization contributions to the alignment associated with a variety of configurations are shown for a number $N=5$ and $N=6$ of nucleons. These systems schematically correspond to the nuclei ^{168}Yb and ^{167}Yb respectively, where the [660] 1/2, [651] 3/2 and [642] 5/2 Nilsson states belonging to the $i_{13/2}$ orbital are occupied, the [642] 5/2 being closest to the Fermi energy.

The equivalence of the NFT treatment of the dealignment induced by the Fock term and the vacuum polarization associated with pairing vibrations, and the standard expression given by eq. (8) is exemplified in fig. 2a. The deviations observed starting at $\omega \sim 0.34$ MeV, are due to the breaking down of the RPA at the transition frequency $\omega = 0.212$ MeV.

In all cases the polarization of the vacuum induced by the pairing force leads to negative contributions, thus dynamically reducing the alignment of the system. The states which are strongest affected are the ones with quantum numbers (+,0) corresponding to configurations where all pairs of particles are coupled in configuration leading to $J^{\pi}=0^{+}$ angular momentum at $\omega=0$, in qualitative agreement with the experimental data [4].

In graph (d) of fig. 2 the quantity $i_0 = (J^{(1)} - J^{(2)})\omega$, which is the value of the alignment determined by extrapolating the local slope $[di/d\omega]_{\omega_0}$ to $\omega=0$, is shown as a function of ω.

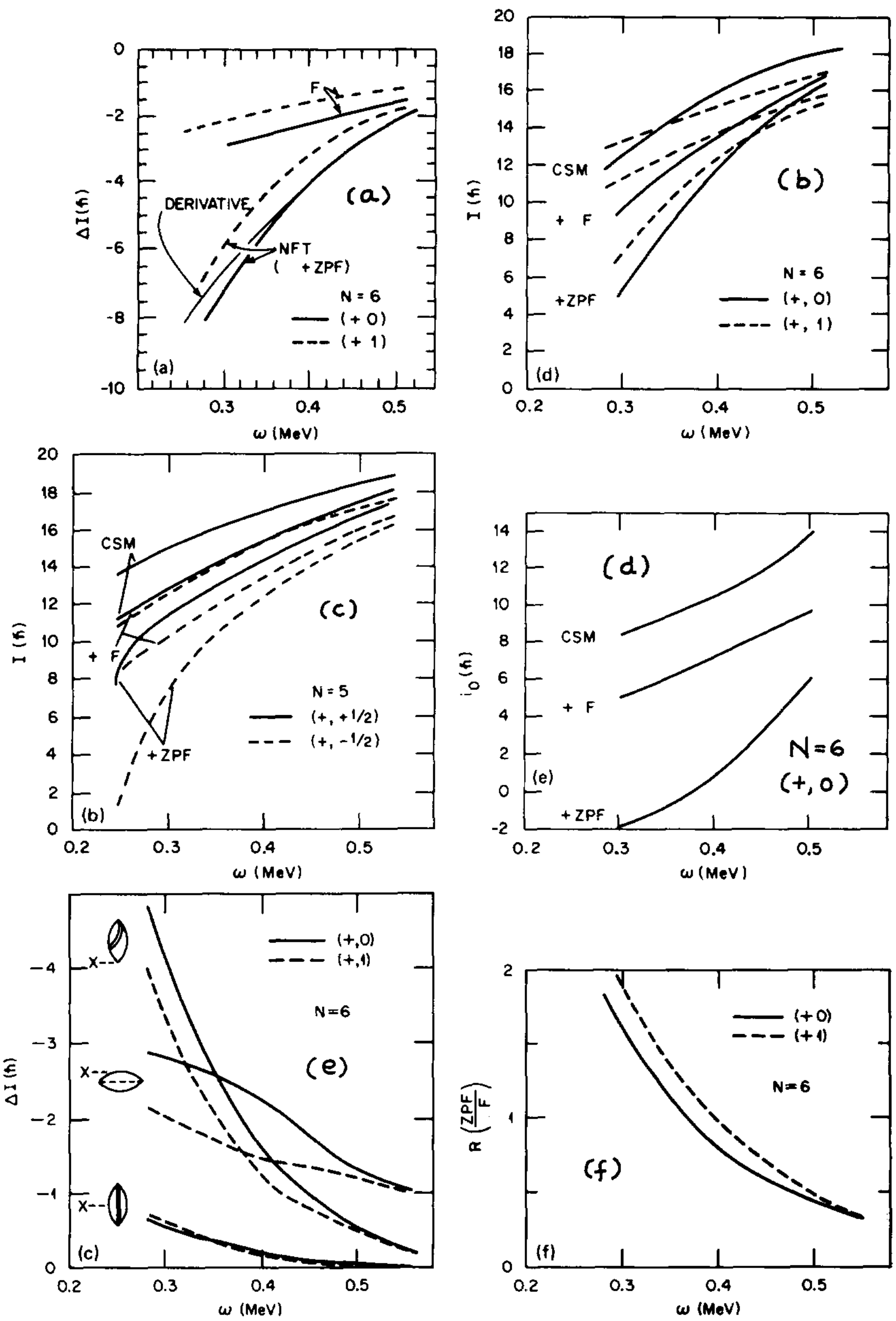

Fig. 2. Dealignments associated with the correlation induced by pairing vibrations. The parameter Q used in the calculations is equal to 1/6 and corresponds to a quadrupole deformation parameter $\beta \sim 0.3$. In (a) the contributions (F) arising from graphs (d) and (e) of fig. 1 and from the zero point fluctuation (ZPF) processes (f)–(m) also of fig. 1 are displayed for $N=6$ particles and for two configurations with parity and signature quantum numbers (+, 0) (full drawn curve) and (+, 1) (dashed curve). Also given is the value of eq. (8) for the (+, 0) configuration as a thin continuous curve. In (b) and (c) the total alignments, summed of the cranked shell model (CSM) the Fock (F) and the zero point fluctuation (ZPF) contributions, are shown for different configurations in both odd ($N=5$) and even ($N=6$) systems. They were constructed by filling the cranked $i_{13/2}$ orbital in such a way that in all cases the lowest-energy state of the given quantum numbers are obtained. In (d) the quantity $i_0=\omega(J^{(1)}-J^{(2)})$ is shown as a function of the rotational frequency. In (e) the Fock, correlation potential and reoccupation diagram contributions are shown for two configurations as a function of the rotational frequency. In (f) the ratio of the summed contribution of the graphs containing a pairing vibration (ZPF) and the Fock (F) contributions, are shown as a function of the rotational frequency for the configuration (+, 0) with $N=6$.

When measured against the cranked shell model result, the value of i_0 associated with the full renormalization (F+ZPF) amounts to ~ 10 units of angular momentum, again in qualitative agreement with the empirical findings [#3] [4,12].

In graph (e) of fig. 2 the value of the different types of processes contributing to the dynamical dealignment are shown as a function of ω. Diagrams of type (j)–(m) (fig. 1) lead to the largest contributions, followed by the Fock graphs (d)–(e) (fig. 1), the smallest contributions arising from graphs (f)–(i) (fig. 1).

The reoccupation correction diagrams (f)–(i) (fig. 1) describe the change in the angular momentum operator (effective spin) due to the presence of pairing vibrations. The correlation potential corrections (j)–(m) (fig. 1) describe the renormalization of the single-particle motion. Within the formalism of Ward's identity [13], graphs (f)–(i) are known as vertex renormalization diagrams and graphs (j)–(m) are known as single-particle renormalization diagrams, and constitute a set of sum-rule conservings graphs. The vertex renormalization graphs give smaller contributions than the single-particle renormalization graphs because of the smaller energy denominators entering in the last type of graphs.

The physical meaning of the three types of processes is again illustrated in graphs (A), (B) and (C) of fig. 1, where they are shown in terms of single-particle self-energy processes. In fact, these graphs are obtained from the closed loop graphs by cutting a fermion to which no external operator is applied.

The process (A) is associated with the Fock contribution of the pairing force to the single-particle motion, and can be viewed as a velocity dependent effective mass (k-mass). On the other hand, graph (C) leads to the ω-dependent effective mass associated with pairing vibrations [14]. Because of the strong non-locality of the pair field, it is not surprising that the process leading to the k-mass can produce contributions which are of the same order of magnitude as the ω-mass type contributions.

The ratio between the summed contributions of diagrams containing phonons and those arising from the pairing mean field are shown in graph (f) of fig. 2. Although all contributions to the dealignment tend to zero for large rotational frequencies, those associated with the average field are more rigid. The value $R(\text{ZPF/F})$ vanishes as $1/\omega^3$, as expected from a simple analytic estimate carried in the two-level model [15].

We conclude that a quantitative description of the dynamical dealignment arising from the dressing of the single-particle motion through fluctuations of the pairing field can be obtained within the framework of the nuclear field theory, making use of second-order vacuum polarization diagrams.

[#3] The comparison of the experimental data for the (+, 0) configuration of ^{168}Yb and a self-consistent calculation carried out according to ref. [2] give, for the difference $(i_0)_{\text{exp}}-(i_0)_{\text{CSM}}$, values of the order of 8–10$\hbar$ [12].

Discussions with Y.R. Shimizu are greatly appreciated. Two of us (F.B. and M.G.) want to acknowledge financial support from the CAICYT (Spain).

References

[1] P.J. Twin, Proc. Intern. Conf. on Nuclear physics, (Florence, 1983), eds. P. Blasi and R.A. Ricci, Vol. II (Compositori, Bologna, 1983) p. 527;
D. Schwalm et al., Frontiers in nuclear dynamics, eds. R.A. Broglia and C.H. Dasso (Plenum, New York, 1985) p. 33.

[2] R. Bengtsson and S. Frauendorf, Nucl. Phys. A 314 (1979) 27, 139;
S. Frauendorf, Nuclear physics, eds. C.H. Dasso, R.A. Broglia and A. Winther (North-Holland, Amsterdam, 1982) p. 111.

[3] F.S. Stephens and R.S. Simon, Nucl. Phys. A 183 (1972) 257;
F.S. Stephens, Frontiers in nuclear dynamics, eds. R.A. Broglia and C.H. Dasso (Plenum, New York, 1983) p. 73.

[4] J.C. Bacelar, M. Diebel, C.E. Ellegaard, J.D. Garrett, G.B. Hagemann, B. Herskind, A. Holm, C.X. Yang, P.O. Tjøm and J.C. Lisle, Proc. Fifth Nordic Meeting on Nuclear physics (Jyväskylä, March 1984) p. 201; and NBI-Oslo-Manchester preprint (1985).

[5] R.A. Broglia, M. Diebel, S. Frauendorf and M. Gallardo, Phys. Lett. B 166 (1986) 252;
Y.R. Shimizu, J. Garrett, R.A. Broglia, M. Gallardo and E. Vigezzi, to be published.

[6] J.L. Egido and P. Ring, Nucl. Phys. A 383 (1982) 189; A 388 (1982) 19; Phys. Lett. B 95 (1980) 331;
J.L. Egido, H.J. Mang and P. Ring, Nucl. Phys. A 334 (1980); A 341 (1980) 229;
U. Mutz and P. Ring, J. Phys. G 10 (1984) L39;
L.F. Canto, P. Ring and J.O. Rasmussen, Phys. Lett. B 161 (1985) 21;
W. Nazarewicz, J. Dudek and Z. Szymanski, Nucl. Phys. A 436 (1985) 139.

[7] R.A. Broglia, Theory of nuclear structure and reactions (La Rabida, Huelva) (World Scientific, Singapore, 1986) p. 133; Nucl. Phys. A 447 (1985) 489c.
[8] D.R. Bes, G.G. Dussel, R.A. Broglia, R. Liotta and B.R. Mottelson, Phys. Lett. B 52 (1974) 253.
[9] D.R. Bes and R.A. Broglia, Nucl. Phys. 80 (1966) 289.
[10] L.A. Goodman, Nucl. Phys. A 230 (1974) 466.
[11] R.A. Broglia, M. Diebel, F. Barranco and S. Frauendorf, XXIII Intern. Winter Meeting on Nuclear physics, Ricerca Scientifica ed Educazione Permanente, Universita di Milano, Supplement No. 4 (1985) p. 1.
[12] J. Garrett, private communication.
[13] J.R. Schrieffer, Theory of superconductivity (Benjamin, New York, 1984).
[14] C. Mahaux, P.F. Bortignon, R.A. Broglia and C.H. Dasso, Phys. Rep. 120 (1985) 1.
[15] D.R. Bes, R.A. Broglia, J. Dudek, J. Szymanski and W. Nazarewicz, Ann. Phys. (NY), to be published.